

Experimental Study on the Impact of Seasonal Sound Speed Variability on Signal Detection Range in Arabian Sea

Elizabeth Shani N.X.,^{#,*} Nimmi R. Nair,[§] R.P. Raju,[§] and R. Sajeev[#]

[#]*Department of Physical Oceanography, School of Marine Science, Cochin University of Science and Technology, Kochi, Kerala - 682016, India*

[§]*DRDO - Naval Physical and Oceanographic Laboratory, Thrikkakara, Kochi, Kerala - 682021, India*

^{*}*E-mail: shany.pisces@gmail.com*

ABSTRACT

Temporal variability of Signal Detection Range (SDR) with respect to measured noise level and sound speed is examined. An N x 2D acoustic model which included bathymetric variations, was used to study detection ranges for an area in Arabian Sea. Azimuthal and seasonal SDR at octave bands within 500 Hz were determined at different receiver depths. Study shows that seasonal change in sound speed profile resulted in high SDR and noise level in winter at the location. Study also confirms the significant seasonal difference in detection range corresponds to the cut off frequency at 160 Hz. Detection range for a receiver at a depth 40 m is observed to be high across the azimuth and seasons of study.

Keywords: Ambient noise; Indian ocean; Seasonal variability; Signal detection range; Transmission loss modeling

1. INTRODUCTION

Sonar equation is the simplest and easiest way to estimate the signal excess (SE) in detection performance of sonar systems. It compares the received level of signal to the background noise level. Analysis of SDR for the design and performance evaluation of sonars is generally based on this sonar equation. In the realm of underwater acoustics, SDR specifies the range up to which target is detected without any discontinuity¹. Hence in target detection, acoustic energy reaching the sonar from the target is to be extracted from the surrounding noise. This background limitation with respect to noise is analyzed by the characteristics of ambient noise or soundscape. Ambient noise is the unwanted background sound after accounting for all the identifiable sources,² whereas the underwater soundscape presents the dynamic spatio-temporal aspects of an acoustic habitat related to the contribution from biotic, abiotic, and anthropogenic sources³⁻⁴. As the sources of noise and environmental conditions are inconsistent, SDR shows spatio-temporal variability in accordance with underwater soundscape and propagation scenario⁵.

The dependence of SDR on environmental conditions is discussed here in terms of Ambient Noise (NL) and Transmission Loss (TL) in sonar equation. Based on the type of sonar system two types of equations are employed to tabulate SE, active and passive equations. In passive systems signal originates at the target and propagates to receiver hence TL is one way whereas in active systems signal originates and propagate back to the

same transmitter after reflecting from the target. Hence TL has to be accounted in two way propagation⁶, as shown below:

$$\text{Passive: } SE = SL - TL - NL - DT \quad (1)$$

$$\text{Active: } SE = SL - 2TL - NL + TS - DT \quad (2)$$

In these equations, SL is the source level of the target to be detected, NL and TL represents the ambient noise level and transmission loss respectively at the location and DT, is the detection threshold. In active sonar equation an additional term TS (target strength) also included and it is measured at 1 m from the acoustic center of the target. The effects of propagating medium conditions on sonar performance is accounted in TL and NL terms

Passive SONAR equation has been exercised as the base for signal detection range estimation. This study also covers the azimuthal and depth wise variation in SDR for predominant seasons, at one-third octave frequencies 63, 100, 160, 250 and 400 Hz. A three dimensional (3D) numerical model⁷ were used to generate the TL variation with respect to the prevailing environment. Very few works⁸ have incorporated such oceanographic parameters in signal detection studies. At any situation, the discrimination of an underwater target highly depend on the propagation characteristics of the medium and the present paper shall highlight these aspects with reference to Indian waters specific to Arabian Sea. Here, such spatio-temporal change in the sonar performance is modeled by inclusion of measured - bathymetry, sound speed profiles and noise levels.

2. EXPERIMENT LOCATION AND MODEL EMPLOYMENT

The study area is a region of tropical shallow water environment off the west coast of India, as shown in Fig. 1(a). It is indicated by a circle of 60 km radius, station depth is 65 m, and the selected area is marked by continental shelf of drastically varying depth. Bathymetry of the location varies from 65 m to 350 m as move away from the shore. However, a uniform bathymetry is observed for along shore propagation⁹.

The landside of study region with respect to north, covers very shallow bathymetry. Hence the TL model domain is restricted to a field from 20° to 220° with a width of 200°. This boundary demarcation has been shown in Fig. 1(a) as lines OA for 20° and OE for 220°. The study area is discretized into 20 radial sectors with 10° azimuthal resolutions. The sector lines are labeled as S-02, S-03, up to S-22 as shown with receiver at the center.

The selected shallow water location has been well studied for different oceanographic features¹⁰⁻¹¹ and it is known for its short term and synoptic variability of upper ocean thermal structure,¹² as discussed in section3.

Transmission loss (TL) term in SONAR equation accounts for the loss of the acoustic energy during its propagation from the source to its receiver position through the medium. Based on the underlying mathematical interpretation of wave equation that controls the propagation, choice of models are used in underwater acoustics¹³⁻¹⁴. The given work on SDR, employed parabolic equation (PE) based range dependent numerical model to simulate the transmission loss with respect to the prevailing environment. PE based on the numerical scheme implicit finite difference called PE-IFD is efficient in handling

range dependent low frequency propagation problems, followed in the work. PE-IFD gives range marching solution to the propagation problem by applying Crank-Nicolson type implementation scheme.¹⁵

3. OCEANOGRAPHIC AND ACOUSTIC DATA

Underwater noise measurements carried out onboard research vessel INS Sagardhwani during 2015-2017 along with sound speed profiles (from CTD casts) were utilized for this study. Sediment type is considered as silty-sand (based on geo-acoustic dataset) with the corresponding compressional speed, attenuation coefficient and density¹⁶.

Figure 1(b) shows the sound speed profiles along three sector lines from the study region, S-06, S-09 and S-11 (as marked in Fig.1(a)) at every 10 km range. Y-axis represents depth of water column, top X-axis stands for sound speed in m/s, and bottom X-axis denotes the radial distance of profiles from receiver location. Bathymetry along each sector line is represented with blue dotted line.

As seen in Fig. 1(b) summer and winter profiles differ in structure. In summer, sound speed level is higher about 3 m/s in the upper layer up to 40 m than winter. But no significant surface duct was seen in summer. In summer, the high sea surface temperature results in very shallow surface duct whereas in winter a well-mixed surface layer develops a deep surface duct. In winter the typical temperature inversion feature, of the south Arabian Sea is a major factor that will affect seasonal acoustic propagation conditions. Thadathil and Shankar¹⁷⁻¹⁸ had observed this temperature inversion in the Arabian Sea coastal waters especially south east coast, and reported that the inversion layer thickness varies from

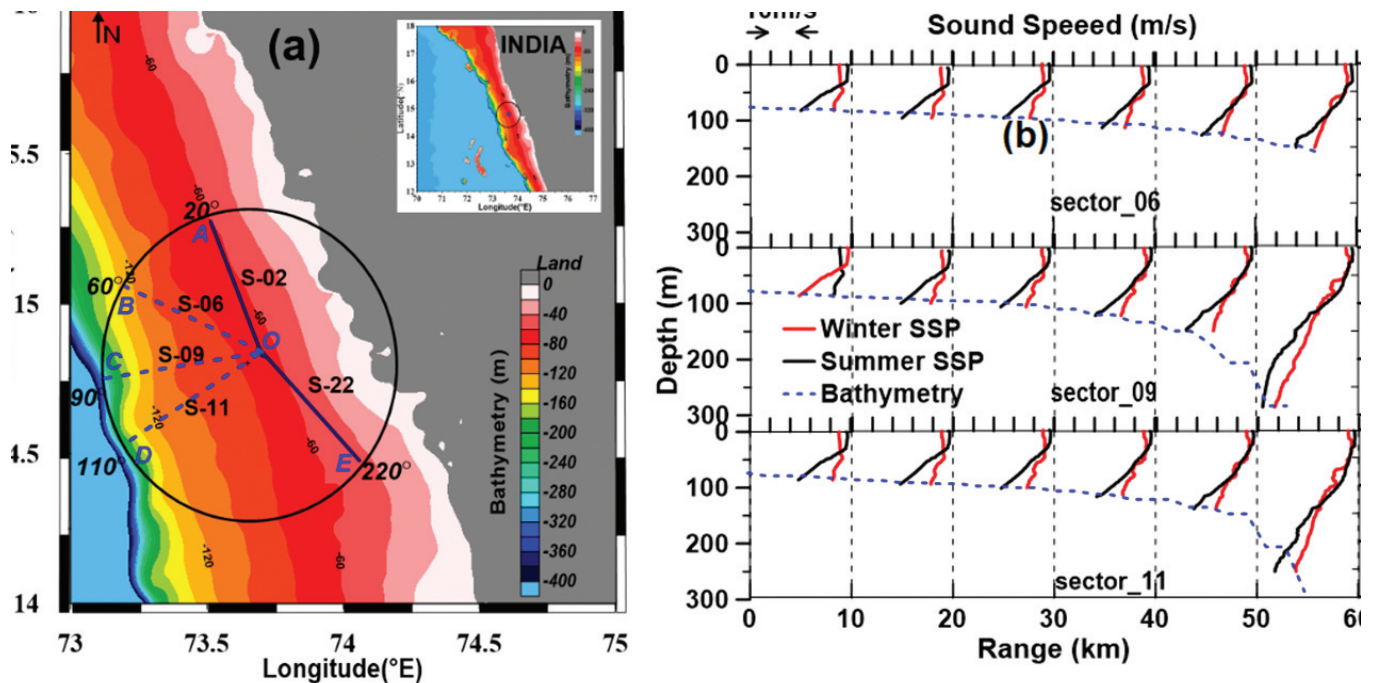


Figure 1. (a) Ambient Noise measurement location-off the west coast of India, and (b) In-situ Sound Speed Profile (SSP) of the location collected during winter (red) and summer (black). Figures are selected from three sectors namely S-06, S-09 and S-11, and profiles are plotted in each 10 km distance from receiver location (O). Blue dotted line shows the bathymetry.

10 to 80 meter with an equivalent gradient of 0.0–1.2 °C/m. However other coastal regions in Arabian Sea also reported with the signature of subsurface maxima that create variability in signal detection with respect to season¹⁹. This surface layer temperature inversion is a stable feature in this area during winter. The given SSP is a representative profile with much extended mixed layer depth and temperature inversion at 42 m depth causes the surface duct. The cut off frequencies²⁰ for winter and summer sound speed profiles are 172 Hz and 2400 Hz respectively. This implies that in summer, the spot frequencies considered will not propagate in the surface duct.

Noise measurements were carried out onboard in silent regime and drift mode. Standard broadband hydrophones, GRASS 10CC were used for measurements (omni-directional up to 20 kHz). Hydrophones were deployed at four depths such as 10 m, 20 m, 30 m and 40 m from surface along with calibrated depth sensors. Noise recording was carried out (sampling frequency = 51.2 kHz) using CRio (National Instruments) DAQ for 15 minutes. Noise level as PSD (Power Spectral Density) was computed for 5 minute data with Hanning window in one-third octave band. The mean noise level for both seasons is derived from 20 datasets of each 5 minute time duration.

Wind speed from onboard AWS (Automatic Weather Station) and marine traffic from AIS (Automatic Identification System) were also recorded around the study area during noise measurements at sea. The 45-minute average wind speed was 14 m/s in summer and 8 m/s in winter season for three years.

Contribution from surface generated sea state noise and traffic induced noise dominates the ambient noise spectrum up to from 20 Hz - 50 kHz. At low frequencies (<500 Hz),

noise spectrum will be dominated by the traffic induced noise and above 500 Hz up to 50 kHz, wind speed is the major contributor to the total noise level. However, in the absence of nearby shipping noise, wind driven noise will dominate the low frequency part of the spectrum especially in shallow water²¹. For this study on noise variability, dataset with no marine traffic in the immediate vicinity (as per AIS) is selected. This low frequency band of traffic noise is selected for this study.

The average PSD of noise data for both seasons at different receiver depths and frequencies are plotted in Fig. 2. The solid circles on the graph show the hydrophone depth and colored lines correspond to frequencies such as 63, 100, 160, 250 and 400 Hz.

Noise variability analysis among the selected frequencies reveals noise level is minimum at 400 Hz at all receiver depths irrespective of season. However, there exists a frequency dependent variation of ambient noise levels between winter and summer. In summer, variation of noise level is uniform at all depths; it decreases with increase in frequency. Such a proportional variation in noise level with respect to frequency is not observed in winter, where the measured noise level is high at 160 Hz and 250 Hz compared to 100 Hz and 63 Hz. In winter, the hydrophones at 20 m and 30 m show higher noise level than the hydrophones at 10 m and 40 m at all selected frequencies. Whereas, in summer it is observed that only 40 m hydrophone has the lowest noise level and other three hydrophones have higher noise levels.

4. METHODOLOGY

As mentioned passive SONAR equation is implemented in SDR estimation, by computing the maximum range at which the signal excess (SE) falls below zero (Array Gain is assumed to be zero), to account for NL in sonar equation, equ (1) at

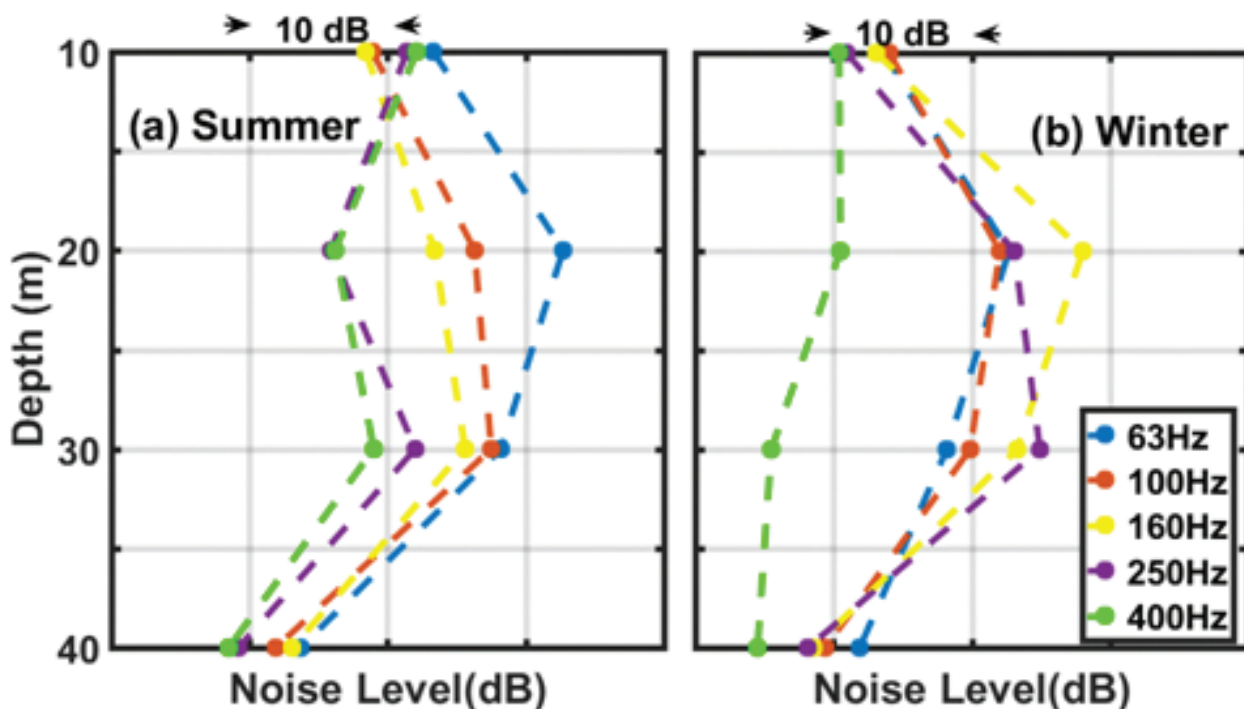


Figure 2. Ambient noise variability across the depths 10, 20, 30 and 40 m in two seasons summer and winter.

each depth an average of measured NL for each season is used in SE computation.

$$SE = SL - TL - NL - DT \tag{3}$$

Considering narrowband passive detection, DT is computed here for Pfa (Probability of false alarm) = 10^{-4} , Pd (Probability of detection) = 90%, $DT = 3.7^{22}$.

A typical large tanker is considered for target detection. The acoustic energy radiated by the vessel exists as a continuous spectrum on which narrowband discrete components are superimposed. Machinery noise and propeller noise dominates the spectrum of radiated noise level of a ship in most conditions.²³ However, for SL estimation ANDES²⁴ model was used in which vessels are classified into 5 divisions based on their type such as Super tanker, large tanker, Tanker, Merchant and Fishing vessel. For each type source level spectra is given for selected frequencies from 5 Hz to 400 Hz. A constant source level of 177 dB with source depth 25 m is used in the SE calculation. Constant source level helps to capture the seasonal variability of signal detection range at different frequencies.

PE models are the best choice for low frequency underwater acoustic propagation studies. In 3D models, complete 3D models and Nx2D models are employed as per the environment and computing complexities requirement. Instead of using complete 3D model in this paper, N x 2D propagation model was used without considering azimuthal coupling. Environmental sampling could not be achieved in fine resolution as needed for 3D model results in same model simulation by 3D and N x 2D models. However using N x 2D model achieved improved computational efficiency without affecting the resolution of model simulation. TL for each range depth grid was computed using PE-IFD. The range dependent environment with respect to the sound speed profile and bathymetry is included as an input to the model,²⁵ and geo-acoustic parameters are kept constant as discussed in section 2. To include the medium properties of respective seasons, in-situ sound speed profiles are used in model. High frequency part of acoustic spectrum is more sensitive to the air sea interactions at the surface boundary, hence loss incurred due to surface scattering have less impact for the frequencies and wind conditions considered here.

5. RESULT

5.1 Modeled TL

The modeled TL for both seasons at five selected frequencies is shown in Fig. 3. The section plots are presented for four receiver depths, 10, 20, 30 and 40 m at which ambient noise measurements are available.

The salient difference between seasons in Fig. 3 is that the TL is higher in summer than winter at all chosen depths and frequencies. This is due to the deep surface duct seen in Fig. 1(b), which is conducive for long range propagation in winter. While in summer, the corresponding sound speed profiles (Fig. 1(b)) are not favorable for ducted propagation and hence energy spreads into deeper waters. The transmission loss at 63 Hz is lowest among the selected frequencies and the corresponding TL mosaic has a concentric circular feature in winter which is prominent at 40 m in Fig. 3. At higher frequencies the circular

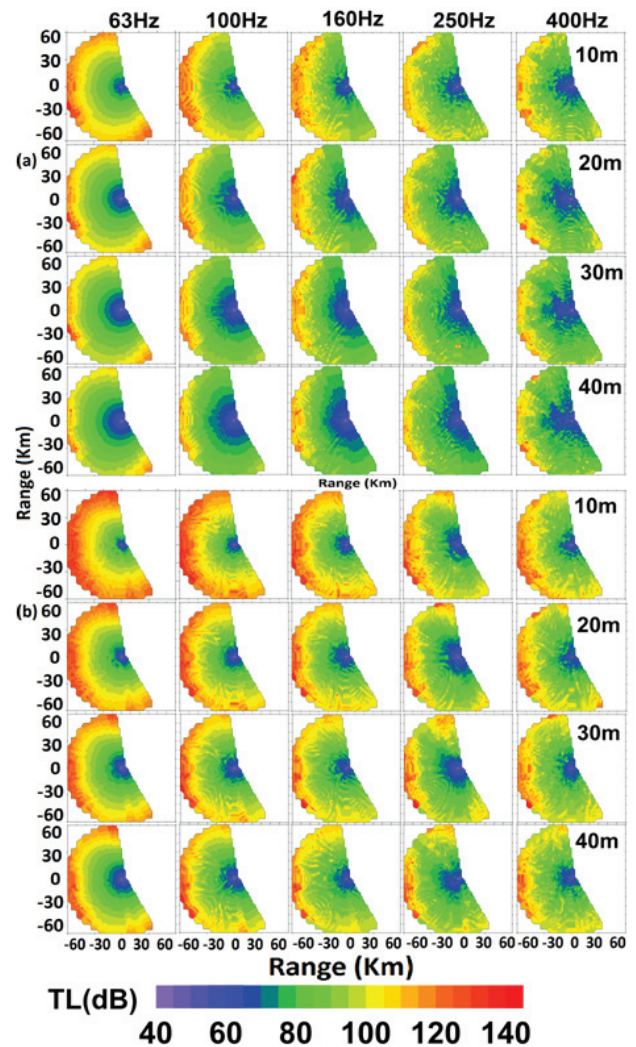


Figure 3. Model predicted TL Mosaic in winter and summer, at five frequencies and four depths.

feature is absent in the TL mosaic.

Figure 4, shows the modeled TL curve at 10 m receiver in summer and winter season. X axis denotes the range in km and Y axis stands for the TL value in dB. In winter TL curve keeps lower level than their summer profile during the entire propagation range at all frequencies. An exception is observed at frequency 160 Hz. As seen in Fig. 4, frequencies above the cutoff which is 170 Hz in winter (discussed in section 3), such as 250 Hz, 400 Hz and 500 Hz all have low TL values than low frequency counterparts.

5.2 Signal Detection Range

The signal detection range is computed by estimating the range above which signal excess becomes zero along each bearing. Figure 5 shows the variability in SDR estimated using equation 1, where radius of the circle stands for the range and sectors denotes the azimuthal direction. Each plot corresponds to signal detection range for a particular frequency and depth in summer (solid line) and winter (dotted line). Frequencies are mentioned at the top of each column and receiver depth on the left side of the plot.

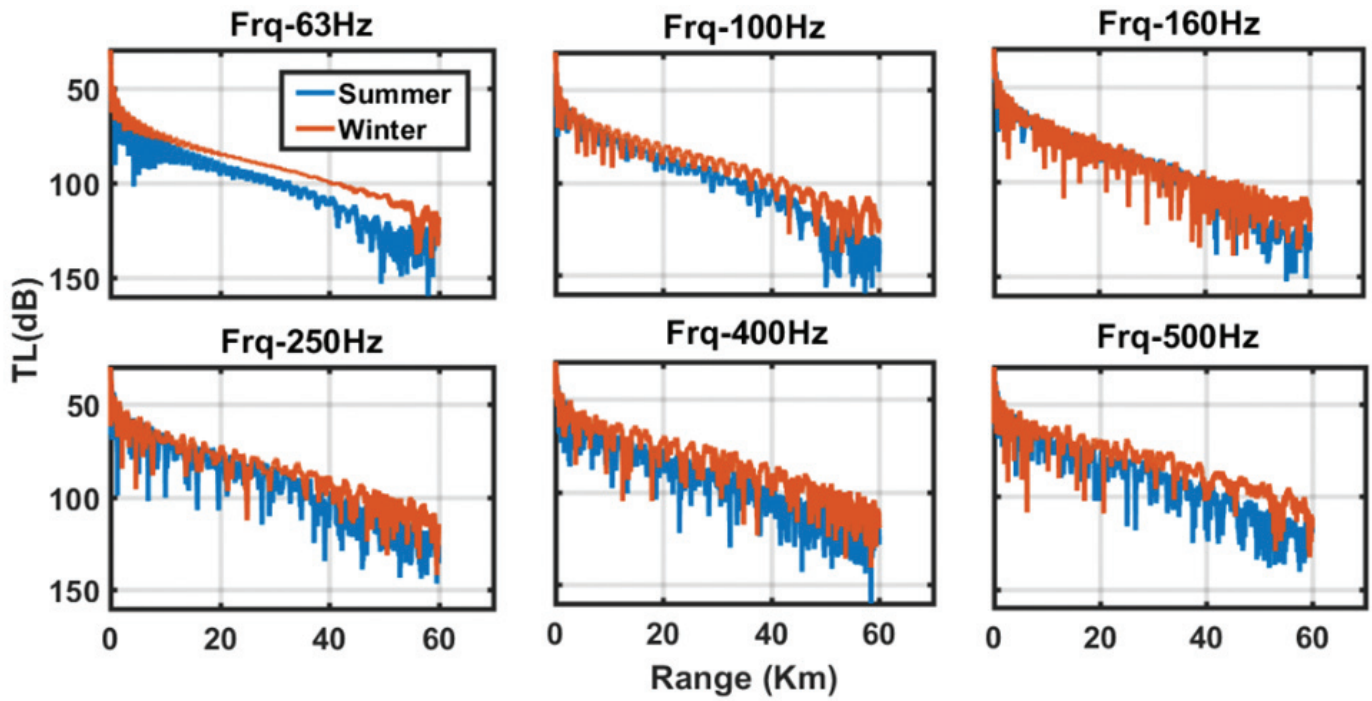


Figure 4. Model predicted TL over the range from source to receiver (60 km) at six frequencies in winter (orange) and summer (blue), receiver depth is 10 m.

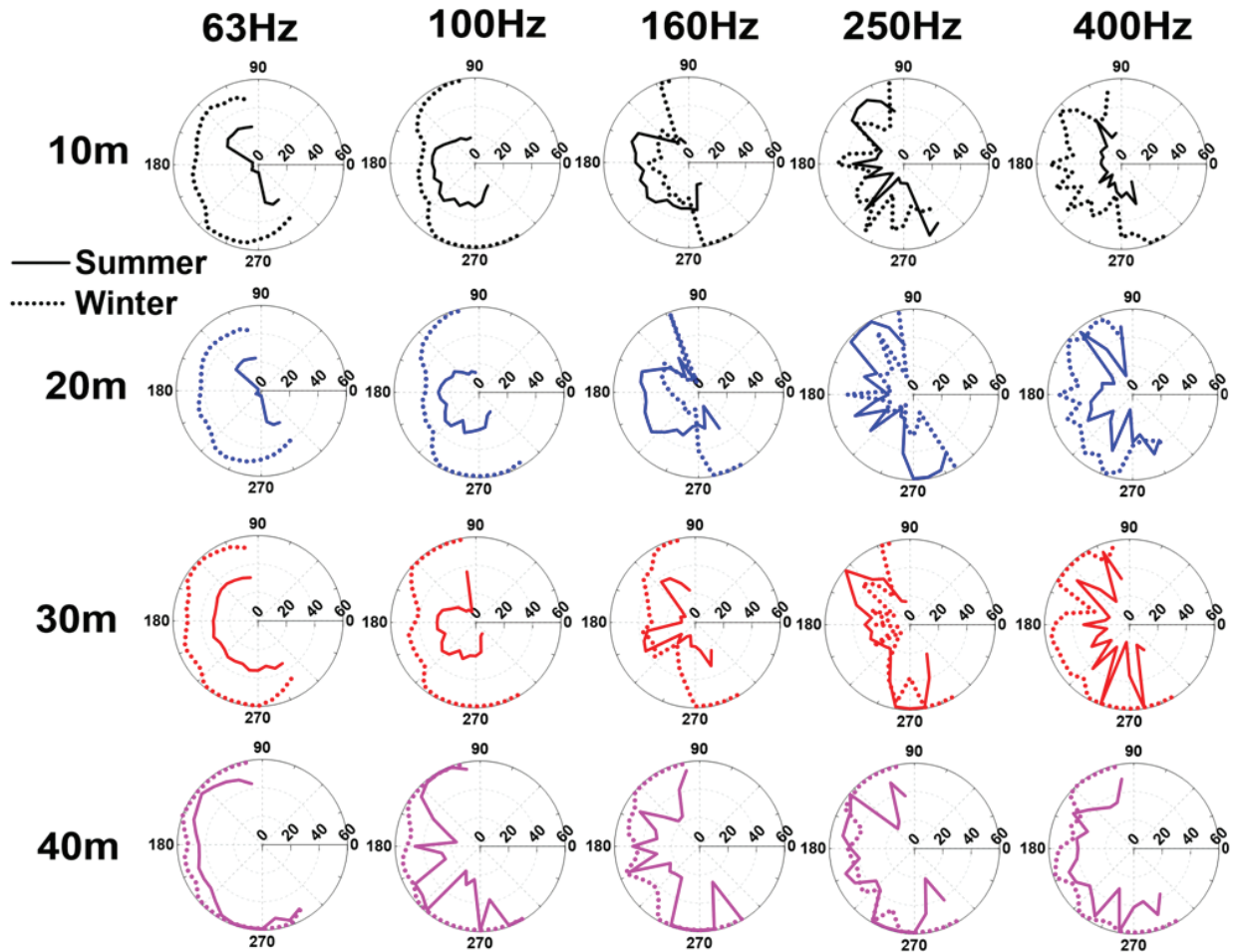


Figure 5. Signal Detection Range (SDR) at 5 selected frequencies and four receiver depths. In each polar plot both summer (solid line) and winter (dotted line) SDR are given.

6. DISCUSSION

The maximum SDR is observed for the deepest receiver at 40 m at all the selected frequencies. The difference between the summer and winter signal detection ranges is minimal at 40 m. SDR is high in winter than summer at all receiver depths and frequencies. The signal detection range peaks along azimuthal directions with steeper down slope bathymetry which is an indication of favorable down slope acoustic propagation. A significant seasonal difference in SDR at 160 Hz is noted from Fig.5, it is higher in summer than winter. The TL values at 160 Hz is observed (Fig. 4) to be almost same in both summer and winter. This result has direct connection with the computed cut off frequency of 172 Hz (winter) which is close to 160 Hz. Hence, seasonal variation of SDR at 160 Hz is due to noise level. From Fig.2 it is seen that in winter maximum ambient noise is observed at 160 Hz and is much higher than in summer. In both winter and summer (Fig. 2), higher noise levels are observed at 20 m and 30 m and their corresponding SDRs are short at these depths.

In winter the lowest SDR was estimated at 160 Hz and 250 Hz, the observed noise level also peaks at these frequencies. In summer, as seen in fig 4, the minimum detection range for 63 Hz is for a receiver at a depth of 20 m; this coincides with the maximum ambient noise level observed at this location. At frequencies 100 Hz, 160 Hz and 250 Hz the lowest detection range is at a depth of 30 m, where maximum noise level is observed at these frequencies. For 400 Hz, the minimum detection range is observed at a depth of 10 m which is consistent with maximum noise level at 10 m. Thus the cumulative effect of ambient noise level and TL results in the observed detection range at all depths and frequencies.

7. CONCLUSION

Signal detection range depends on both ocean acoustic and environmental conditions. The deepest receiver at 40 m corresponds to highest signal detection range along all azimuths. At 40 m, the selected frequencies are unaffected by any seasonal change. This is consistent with corresponding seasonal observations in NL and modeled TL values. The signal detection range is always high in winter than summer with the exception of 160 Hz, where it is reversed. In winter, where the cut off frequency is 172 Hz, minimum detection range is observed at 160 Hz. In summer and winter, ambient noise level is found to be higher at 20 m and 30 m. The estimated SDR also shows shortest range at these depths. Further experimental studies on azimuthal variation in SDR are planned in future.

ACKNOWLEDGMENT

The authors would like to thank Director, NPOL, DRDO for the encouragement to do this work. Authors also thank the scientists and the technical team of the Ocean Science group at NPOL for the support provided in conducting the experiments over the years to collect noise and environmental data. Authors express their acknowledgment to Mr. P V Nair for his guidance. This work is funded by DRDO, Ministry of Defence, India, under its research fellowship scheme.

REFERENCES

1. Miksis-Olds, J.L.; Vernon, A. & Heaney, K.D. The Impact of Ocean Sound Dynamics on Estimates of Signal Detection Range. *Aquatic Mammals*, 2015, **41**(4), 444-454. doi:10.1578/AM.41.4.2015.444.
2. Wenz, G.M. Acoustic ambient noise in the ocean: spectra and sources. *J. Acoust. Soc. Am.*, 1964, **34**(12), 1936-1956. doi: 10.1121/1.1909155.
3. Duarte, C.M; Chapuis, L.; Collin, S. P.; Costa, D.P.; Devassy, R.P; Eguiluz, & V.M.; *et al.* The soundscape of the Anthropocene Ocean. *Science*, 2021, **371**(6529). doi: 10.1126/science.aba4658
4. Slabbekoorn, H. & Niels, B. Soundscape orientation: A new field in need of sound investigation. *Animal Behaviour*, 2008, **76**(4). doi:10.1016/j.anbehav.2008.06.010.
5. Tyler A.H.; Gerald, L.D.; John, A.H. & Gregory, S.C. Site specific probability of passive acoustic detection of humpback whale calls from single fixed hydrophones. *J. Acoust. Soc. Am.*, 2013, **134**(3), 2556–2570. doi.org/10.1121/1.4816581.
6. Hodges, R.P. Underwater acoustics analysis, design and performance of sonar. 1st ed. John Wiley & Sons, Ltd., UK. 2010. 17-21 p.
7. Lee, D. & Schultz, M.H. Numerical Ocean Acoustic Propagation in three dimension. World Scientific, Singapore. 1995.
8. Samaran, F.; Adam, O. & Guinet, C. Detection range modelling of blue whale calls in Southwestern Indian Ocean. *Appl. Acoust.*, 2010, **71**(11), 1099-1106. doi: 10.1016/j.apacoust.2010.05.014
9. Chakraborty, B.; Karisiddaiah, S.M.; Menezes, A.A.A.; Haris, K.; Gokul, G.S.; Fernandes, W.A. & Kavitha, G. Characterizing slope morphology using multifractal technique: A study from the western continental margin of India. *Natural Hazards*. 2014, **73**(2), 547-565. doi.org/10.1007/s11069-014-1085-8.
10. Sanilkumar, K.V.; Hareeshkumar, P. V. & Radhakrishnan, K.G. Oceanographic features and their influence on acoustic propagation: Case studies. In Proceedings of ICONS-International conference on sonar- sensors and systems 2002, India, 2002, 577-582.
11. Hareesh kumar, P.V. & Radhakrishnan, K.G. Transmission loss variability associated with up welling and downwelling off the southwest Coast of India. *Def. Sci. J.*, 2010, **60**(5), 476-482. doi: 10.14429/dsj.60.570.
12. Hareesh kumar, P.V.; Pradeep kumar, T.; Mathew, B. & Joseph, M.X. Upper ocean thermal structure off Karwar (West coast of India) during the withdrawal phase of monsoon-1987. *Ind. J. Mar. Sci.*, 1990, **19**, 36-41.
13. Etter, P.C. Underwater Acoustics Modeling and Stimulation. 3rd ed. Spon Press, Taylor & Francis Group, New York. 2003.
14. Jensen, F.B.; Kuperman, W.A.; Porter, M.B. & Schmidt, H. Computational ocean acoustics. Ed. 2. Springer, New York, 2011. 476-536.
15. Lee, D. & McDaniel, S.T. Ocean acoustic propagation by finite difference methods. Pergamon, Oxford, 1988.

16. Chakraborty, B.; Mahale, V.; Navelkar, G.; Rao, B. R.; Prabhudesai, R. G.; Ingole, B. & Janakiraman, G. Acoustic characterization of seafloor habitats on the western continental shelf of India. *ICES. J. Mae. Sci.*, 2007, **64**(3), 551-558.
doi: 10.1093/icesjms/fsl043.
17. Thadathil, P. & Gosh, A. K. Surface Layer Temperature Inversion in the Arabian Sea during winter. *J. Oceanogr.*, 1992, **48**, 293- 304.
doi.org/10.1007/BF02233989.
18. Shankar, D.; Gopalakrishna, V.V.; Sheno, S.S.C.; Durand, F.; Shetye, S. R.; Rajan, C.K.; Johnson, Z.; Araligid, N. & Michael, G. S. Observational evidence for westward propagation of temperature inversions in the southeastern Arabian Sea. *Geophys. Res. Lett.*, 2004, **31**(8), L08305(1-4).
doi: 10.1029/2004GL019652.
19. Abdul, A.S.; Revichandran, C.; Muraleedharan, K.R.; Sebin, J.; Seena, G.; Ravikumar, C.N.; & Manju, G. Sound speed variation in the coastal waters off Cochin and signature of subsurface maxima. *Ocean Dynamics*, 2021, **71**, 923-933.
doi: 10.1007/s10236-021-01472-x.
20. Kibblewhite, A.C. & Denham, R.N. Experiment on Propagation in Surface Sound Channel. *J. Acoust. Soc. Am.*, 1965, **38**(63), 63–71.
doi: 10.1121/1.1909617.
21. Poikonen, A. & Madekivi, S. Wind generated ambient noise in a shallow brackish water environment in the archipelago of the Gulf of Finland. *J. Acoust. Soc. Am.*, 2010, **127**(6), 3385–3393.
doi: 10.1121/1.3397364.
22. Burdic, W.S. Underwater Acoustic System Analysis. Ed. 2. Prentice Hall, Englewood cliffs, New Jersey, 1991. 424-428.
23. Lurton, X. An introduction to underwater acoustics principles and applications. Springer, New York, 2002.
24. Pflug, L. A. & Hall, T. Dynamic ambient noise model (DANM) evaluation using port everglades data. Report No. NRL/FR/7185-04-10064, 2004.
25. Raju, R.P.; Anand, P.; Fernandez, D.R. & Rao, A.R. Effect of azimuthal asymmetry caused by upwelling on 3D ocean acoustic propagation. *Def. Sci. J.*, 2019, **69**(2), 136-141.
doi: 10.14429/dsj.69.14220.

CONTRIBUTORS

Ms Elizabeth Shani N.X. obtained MTech in Ocean Technology from Cochin University Science and Technology (CUSAT), Kochi and currently pursuing PhD at CUSAT, and she was research fellow at DRDO-Naval Physical and Oceanographic Laboratory, Kochi. Her research areas include analysis of ambient noise and the governing oceanographic parameters for its variability, and marine traffic ambient noise model.

In the current study, she conceptualized the work and also carried out noise data analysis, model implementation, and paper writing.

Dr Nimmi R. Nair obtained Masters and PhD from Cochin university of Science and Technology, Kochi. She has acquired AMIE in Electronics and communication. Presently working as Scientist 'F' in DRDO - Naval Physical and Oceanographic Laboratory, Kochi.

In the current work she supervised the work and was also instrumental in collecting noise data and its processing and analysis.

Mr R.P. Raju obtained MSc (Physics) from University of Mysore. Presently he is working as a Scientist 'E' at DRDO -Naval Physical and Oceanographic Laboratory, Kochi. His research areas include SONAR based Ocean acoustic modelling and acoustic model-based signal processing. He is a life member of Acoustical Society of India. In this present work, he guided in the model implementation and supported in preparing model relevant parameters.

Dr R. Sajeer obtained Masters and PhD from Cochin university of Science and Technology, Kochi. He is HOD and Associate professor in the Department of Physical Oceanography, CUSAT. He has 60 publications to his credit. His research areas include: Coastal oceanography, coastal process and fishery oceanography. He had successfully guided 5 PhD students and many students for their MSc and MTech project dissertations.

In the present work, he was involved in planning and execution of the experiment and also gave guidance on the oceanographic data processing relevant to the model.